Dalton Transactions

Accepted Manuscript

This is an *Accepted Manuscript*, which has been through the Royal Society of Chemistry peer review process and has been accepted for publication.

Accepted Manuscripts are published online shortly after acceptance, before technical editing, formatting and proof reading. Using this free service, authors can make their results available to the community, in citable form, before we publish the edited article. We will replace this *Accepted Manuscript* with the edited and formatted *Advance Article* as soon as it is available.

You can find more information about *Accepted Manuscripts* in the Information for Authors.

ROYAL SOCIETY OF CHEMISTRY

www.rsc.org/dalton

Journal Name

Dalton Transactions

Dynamic Article Links ►

Cite this: DOI: 10.1039/c0xx00000x

www.rsc.org/xxxxxx

ARTICLE TYPE

Dinitrosyliron Complex $[Fe_4(\mu_3\text{-}S)_2(\mu_2\text{-}NO)_2(NO)_6]^{2-}$ Containing Bridging Nitroxyls: ^{15}N (NO) NMR Analysis of the Bridging and Terminal NO-Coordinate Ligands

Shih-Wey Yeh,[a] Chih-Chin Tsou,[a] Wen-Feng Liaw*[a]

Received (in XXX, XXX) Xth XXXXXXXXX 20XX, Accepted Xth XXXXXXXXX 20XX
DOI: 10.1039/b000000x

The fluxional terminal and semibridging NO-coordinate ligands of DNIC $[Fe_4(\mu_3\text{-}S)_2(\mu_2\text{-}NO)_2(NO)_6]^{2-}$, a precursor of Roussin's black salt (RBS), are characterized by IR ν(NO), ^{15}N(NO) NMR and single-crystal X-ray diffraction.

Nitric oxide has been identified as a signaling molecule participating in diverse physiological functions through interaction with NO-responsive targets.[1] Iron-sulfur clusters [Fe-S] were known to be the pivotal prosthetic groups targeted by NO.[2] The reported nuclear resonance vibrational spectroscopy (NRVS) and EPR-spectroscopic studies reveal that the major products in nitrosylating specific [Fe-S] proteins are the diamagnetic species, e.g. Roussin's red ester (RRE), Roussin's red salt (RRS) or Roussin's black salt (RBS), in addition to dinitrosyliron complex (DNIC) with characteristic EPR signal g_{av} = 2.03.[3] Also, RBS was characterized as the predominant product upon adding NO to a mutant [4Fe-4S] ferredoxin from *Pyrococcus furious* by using NRVS.[3b] Recently, on the basis of resonance Raman and low-temperature photolysis FTIR data, the diferrous site of an FMN-free FDP (flavodiiron protein) from *Thermotoga maritima* (*Tm* deflavo-FDP) triggering turnover of 2NO to N_2O via a NO-semibridging $Fe^{II}(\mu\text{-}NO)Fe^{III}$ intermediate was proposed.[4] In the synthetic model, $\{Fe(NO)_2\}^9$ thiolate-containing DNICs converted back to [4Fe4S] clusters via a reassembling processes (DNIC → RBS → $[Fe_4S_4(NO)_4]^{2-}$ → [4Fe-4S] cluster) and transformation of $\{Fe(NO)_2\}^9$ DNICs into [2Fe2S] clusters mediated by RRS were demonstrated.[5] In contrast to the inertness of $[Fe_2(\mu_2\text{-}S)_2(NO)_4]^{2-}$ (RRS) toward alkaline medium, RRS readily transforms into the various polynuclear clusters ($[Fe_4(\mu_3\text{-}S)_3(NO)_7]^-$ (RBS), $[Fe_5(\mu_3\text{-}S)_4(NO)_8]^-$, and $[Fe_7(\mu_3\text{-}S)_6(NO)_{10}]^-$) via the proposed protonated intermediate $[Fe_2(\mu_2\text{-}SH)_2(NO)_4]$ in acidic condition.[1b] In this report, complex $[Fe_4(\mu_3\text{-}S)_2(\mu_2\text{-}NO)_2(NO)_6]^{2-}$ (**1**) with semi-bridging nitroxyls acting as a key intermediate in the transformation of RRS into RBS via the assembling process RRS → complex **1** → RBS was reported. The IR ν(NO) and ^{15}N (NO) NMR spectra implicate that complex **1** is fluxional, scrambling terminal and bridging NO ligands at 320 K. In particular, ^{15}N (NO) NMR chemical shift serving as an efficient tool to discriminate terminal and bridging NO-coordinate ligands was demonstrated.

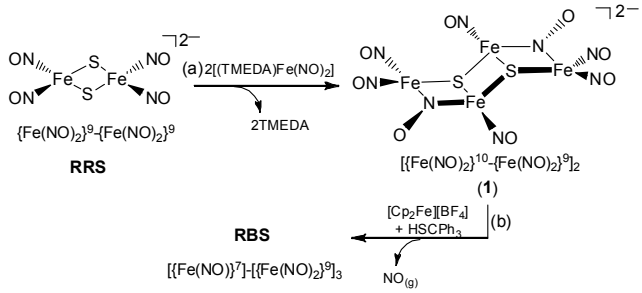

Scheme 1 Conversion pathway from **RRS** to **RBS** via complex **1**.

The reaction of $[Fe_2(\mu_2\text{-}S)_2(NO)_4]^{2-}$ with two equiv of $\{Fe(NO)_2\}^{10}$ DNIC $[(TMEDA)Fe(NO)_2]$ (TMEDA = tetramethylethylenediamine) in CH_3CN affords $[Fe_4(\mu_3\text{-}S)_2(\mu_2\text{-}NO)_2(NO)_6]^{2-}$ (**1**) bearing bridging and terminal NO ligands, characterized by IR, UV-vis, SQUID, ^{15}N NMR and single-crystal X-ray diffraction (Scheme 1a). The reaction is presumed to proceed via coordinative association of $[(TMEDA)Fe(NO)_2]$ and RRS accompanied by release of the labile TMEDA ligand. The straightforward conversion of RRS into complex **1** was monitored by the IR ν_{NO} (1742 w, 1701 s and 1668 m cm^{-1} (CH_3CN)). With the aid of isotopic labeling experiments, the reaction of CH_3CN solution of $[(TMEDA)Fe(^{15}NO)_2]$ and $[Fe_2(\mu_2\text{-}S)_2(^{14}NO)_4]^{2-}$ in a 2:1 molar ratio yielded semi-enriched $[Fe_4(\mu_3\text{-}S)_2(^{14}NO)_4(^{15}NO)_4]^{2-}$ (**1-^{15}NO**) identified by the characteristic IR ν_{NO} spectrum (ν_{NO}: 1721 br, 1685 sh, 1657 vs, 1638 sh, 1510 w and 1483 m cm^{-1} (KBr)), compared to ν_{NO} (1739 w, 1702 sh, 1685 vs, 1668 s and 1510 m cm^{-1} (KBr)) for complex **1** (Supporting Information (SI) Figure S1). The magnitude of ~27 cm^{-1} of the isotopic shift from 1510 cm^{-1} (μ-NO) to 1483 cm^{-1} (μ-^{15}NO) is consistent with the calculated position, based only on the difference in masses between ^{14}NO and ^{15}NO.[5c] The IR ν(NO) spectra suggest that complex **1** is fluxional, scrambling terminal and bridging NO ligands at room temperature. This point has received further support in the study of temperature-varied ^{15}N NMR of complex **1**. As shown in Figure 1a, the ^{15}N (NO) NMR

[a] *Department of Chemistry, National Tsing Hua University, Hsinchu 30013, Taiwan. Fax: +886-3-5711082; Tel: +886-3-5715131 ext 35663; E-mail: wfliaw@mx.nthu.edu.tw*

† Electronic Supplementary Information (ESI) available: Experimental details, crystal data (CCDC-974703), computational details, SQUID, cyclic voltammogram, and IR. See DOI: 10.1039/b000000x/

spectra showing one broad signal (δ 58.3 ppm vs. $MeNO_2$) in the NO region also support that complex **1** is fluxional, scrambling terminal and bridging NO ligands in d_6-acetone at 320 K. Interestingly, complex **1** exhibits a diagnostic ^{15}N (NO) NMR spectrum with bridging NO resonances (δ 200.8 and 200.1 ppm vs. $MeNO_2$) well-removed from the terminal NO resonances (δ 79.7, 73.5, 43.9, 30.3, 27.1 and 21.9 ppm) at 220 K (Figure 1d). As elucidated by Mason and co-workers, the bent nitrosyl possessing lower n_N-π^* excitation energy and the greater imbalance of charge in valence shell giving much larger deshielding displays the downfield chemical shift (in the range of 300-900 ppm) in the ^{15}N NMR, compared to that of the linear nitrosyl (in the range of 20-200 ppm).[6] The presence of two sets of ^{15}N (NO) NMR peaks (δ 200.8, 79.7, 43.9, 21.9 ppm and δ 200.1, 73.5, 30.3, 27.1 ppm with 3:1 ratio, which are integrated on the basis of the similar environment of individual ^{15}NO displaying similar relaxation mechanism in the ladder and boat forms) in complex **1** might be interpreted either as equilibrium isotope effects or as two isomeric forms (ladder-form and presumably, boat-form (inset of Figure 3).[6] The later is preferred due to the significant difference in ^{15}N chemical shift of the two species. It is noticed that the ^{15}N NMR spectrum of complex **1** at 220 K displays δ 79.7, 73.5, 43.9, 30.3, 27.1 and 21.9 ppm (terminal ^{15}NO) in d_6-acetone falling within the range of δ -7.8~25.0 ppm and δ 23.1~76.1 ppm, the characteristic ^{15}N NMR chemical shift of $\{Fe(NO)_2\}^{10}$ and $\{Fe(NO)_2\}^9$ DNICs, respectively.[7] Compared to RRS displaying two absorption bands at 264 and 378 nm in the UV-vis spectrum,[5b] complex **1** shows absorption bands at 273, 343 and 478 nm.

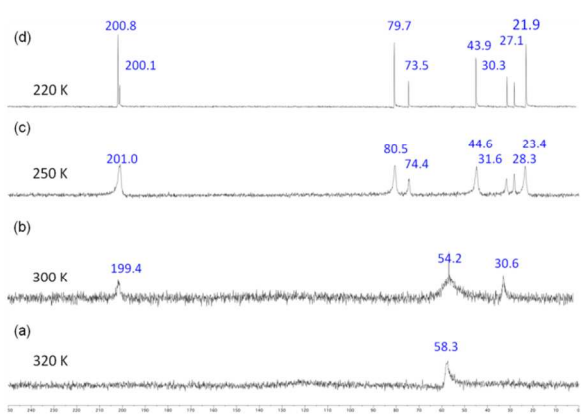

Fig. 1 ^{15}N-NMR spectra of complex **1** in d_6-acetone at (a) 320 K, (b) 300 K, (c) 250 K and (d) 220 K, respectively.

Single-crystal X-ray structure of $[Fe_4(\mu_3\text{-}S)_2(\mu_2\text{-}NO)_2(NO)_6]^{2-}$ unit in K^+-18-crown-6-ether salt is depicted in Figure 2 and selected bond dimensions are presented in the figure caption. The molecule is symmetrical because of a crystallographically imposed inversion center. The unique ladder-shaped structure is constructed by one RRS $[Fe_2(\mu\text{-}S)_2(NO)_4]$ moiety coordinated by two $[Fe(NO)_2]$ motifs. The Fe(1)···Fe(1^i) distance of 2.740(1) Å is longer than the Fe···Fe bond distance of RRS (2.678 Å), and the relatively short Fe(1)···Fe(2) distance of 2.573(1) Å suggests the stronger Fe···Fe interaction. The bridging N(2)—O(2) bond length of 1.224(4) Å (the bond angles Fe(1) — N(2) — O(2) 138.8(3)° and Fe(2)—N(2)—O(2) 131.0(3)°) is comparable to the

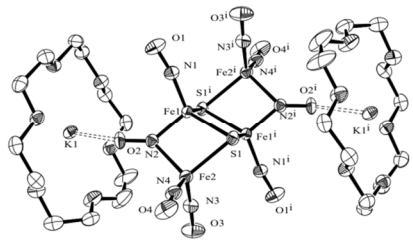

Fig. 2 Molecular structure of complex **1**. Selected bond distances (Å) and angles (deg): Fe(1)…Fe(2) 2.573(1); Fe(1)…Fe(1^i) 2.740(1); K(1)…O(2) 2.777(3); Fe(1)-N(1) 1.660(3); Fe(1)-N(2) 1.761(3); Fe(2)-N(2) 1.967(3); Fe(2)-N(3) 1.676(4); N(1)-O(1) 1.184(4); N(2)-O(2) 1.224(4); N(3)-O(3) 1.182(5); N(4)-O(4) 1.181(4); Fe(1)-N(1)-O(1) 170.2(3); Fe(1)-N(2)-O(2) 138.8(3); Fe(2)-N(2)-O(2) 131.0(3).

N—O bond distance of 1.26 Å in NO^- and the N—O distance of 1.330 (12) Å (the bent Fe — N — O) in $[Fe(NO)_4]^-$.[8] Of importance, the difference of bond distances between Fe(1)—N(2) (1.761(3) Å) and Fe(2)—N(2) (1.967(3) Å) suggests that the Fe(1) center in complex **1** would retain a $\{Fe(NO)_2\}^9$ core and Fe(2) permit a semibridging interaction of N(2)O(2) within $[(NO)Fe(\mu\text{-}NO)Fe(NO)_2]$ unit. This N(2)O(2) polarization may be promoted by a semibridging electrostatic interaction with the immediate vicinity $\{Fe(NO)_2\}^{10}$ motif. This type of interaction may increase the nucleophilicity of semibridging NO, as is evidenced from site-selective interaction of K^+ at the bridging nitroxyl oxygen (Figure 2). The 150 cm^{-1} decrease in ν(NO) (RRS vs. semi-bridging NO of complex **1**) is believed to reflect the strong electron donation from electron-rich $\{Fe(NO)_2\}^{10}$ motif to N(2)—O(2), thereby weakening both Fe(1)—N(2) and N(2) — O(2) bonds and lowering the corresponding stretching frequency. Interestingly, the semi-bridging-NO stretching frequency (1510 cm^{-1} (KBr)) of complex **1** is comparable to that of a semibridging interaction of NO within $[Fe^{II}\text{-}\{Fe(NO)\}^7]$ unit, observed in Hr(NO) (mononitrosyl adduct of nonheme diiron protein hemerythrin) (1658 cm^{-1} (H_2O)) and FDP(NO) (1681 cm^{-1} (H_2O)).[4] In addition, the terminal N—O bond lengths (N(1)—O(1) 1.184(4), N(3)—O(3) 1.182(5) and N(4)—O(4) 1.181(4)) of complex **1** are comparable to the range [1.184(2)-1.187(3) Å] of the $\{Fe(NO)_2\}^{10}$-$\{Fe(NO)_2\}^9$ reduced-form dinuclear DNICs.[9] Therefore, the electronic structure of complex **1** may be best described as coordinative assembly of two fully delocalized $[\{Fe(NO)_2\}^9\text{-}\{Fe(NO)_2\}^{10}]$ motifs. As is evidenced from IR ν_{NO} spectrum (1510 cm^{-1}), the bent Fe—N—O bond angle (Fe(1)—N(2)—O(2) 138.8(3)° and Fe(2)—N(2)—O(2) 131.0(3)°) as well as the relative long N — O bond distance (1.224(4) Å), the electronic structure of the bridging NO closely approaches nitroxyl anion (NO^-).[8]

In order to gain more information about possible isomers of complex **1**, density functional theory (DFT) computation with BP86 functional[10] and a mixed basis set of SDD ECP[11] on Fe and 6-311++G(d,p)[12] on all other atoms were employed on ladder-form **A** and boat-form **B** (inset of Figure 3).[13] On the basis of the experimental and computational parameters summarized in Table S1, the geometric parameters and nitroxyl vibrational frequencies of ladder-form **A** are well comparable to those of complex **1**. The

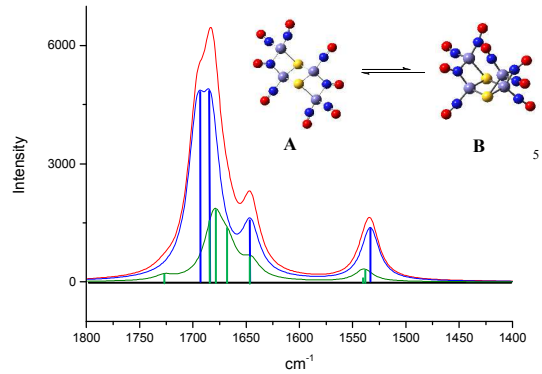

Fig. 3 The calculated vibrational spectra for ladder-form **A** (blue line), boat-form **B** (green line), and the combination of forms **A** and **B** (3 : 1 ratio) (red line).

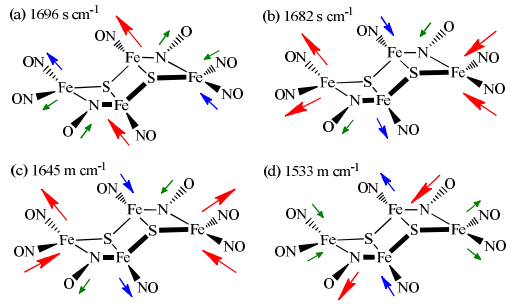

Chart 1 NO vibrational modes of ladder-form **A**.

boat-form **B** is unstable compared to the ladder-form **A** by 1.7 kcal/mol (1.8 kcal/mol) in gas phase at 220 K (298 K). The ^{15}NO-enriched boat-form **B-^{15}NO** is found to be slightly unstable than the ^{15}NO-enriched ladder-form **A-^{15}NO** by only 0.6 kcal/mol (0.7 kcal/mol) in the solvation of acetone at 220 K (298 K), which corresponds to an equilibrium constant $K_{B/A}$ ~ 0.36 (0.31). Interestingly, this value is consistent with the 3:1 ratio of two isomeric **1-^{15}NO** observed in ^{15}N NMR spectra (Figure 1 and inset of Figure 3). The calculated IR spectrum of comformation **A** displays four active NO vibrational frequencies at 1696, 1682, 1645 and 1533 cm^{-1}, which mainly correspond to the anti-symmetric stretching vibrations of two central Fe-terminal NO motifs (Chart 1a), the two anti-symmetric stretching vibrations of two $\{Fe(NO)_2\}$ motifs (Chart 1b and c), and the anti-symmetric stretching vibrations of two Fe_2-semibridging NO motifs (Chart 1d), respectively. In the boat-form **B**, seven active NO vibrational frequencies were calculated to be 1726, 1682, 1678, 1667, 1645, 1540 and 1538 cm^{-1}. The detailed vibrational modes are delineated in SI Chart S1. As shown in Figure 3, the combined calculated spectrum from 3**A** : 1**B** ratio, displaying a similar pattern to experimental IR spectrum of complex **1** (SI Figure S1), also supports two different isomers of complex **1** with 3 : 1 ratio in the ^{15}N NMR at 220 K.

The paramagnetic broadening of ^{15}N NMR peak of NO groups at 300 K (or 250 K) (Figure 1) suggest that the singlet-ground-state complex **1** has a low-lying triplet excited state with small thermal population. In order to estimate the singlet/triplet energy splitting ($\Delta_{S/T}$), the magnetic susceptibility measurement of powdered sample of complex **1** was collected in the temperature range of 2-300 K at 0.5 T. The temperature-dependent effective magnetic moment decreases from 0.666 μ_B at 300 K to 0.201 μ_B at 2 K (SI Figure S2). The best fit to the data indicates that the low-lying triplet excited state is higher than the singlet ground state about 1843 ± 2 cm^{-1} with g value for $[\{Fe(NO)_2\}^9$-$\{Fe(NO)_2\}^{10}]$ fixed to 1.997 (R^2 = 0.991 and TIP = (141.6 ± 3.3) × 10^{-6} cm^3 mol^{-1}) (SI Figure S3). Complex **1**, measured in CH_3CN with 0.1 M $[^nBu_4N][PF_6]$ as supporting electrolyte at room temperature (scan rate 0.5 V/s), displays a reversible redox wave at $E_{1/2}$ = -1.72 V (vs Cp_2Fe/Cp_2Fe^+) with ΔE_p = 150 mV and i_{pa}/i_{pc} = 0.92 (SI Figure S4). The redox potential of -1.72 V (vs Cp_2Fe/Cp_2Fe^+) for complex **1** lies between that of RRS (-2.26 V vs Cp_2Fe/Cp_2Fe^+) and that of RRE $[(NO)_4Fe_2(\mu\text{-SEt})_2]$ (-0.95 V vs Cp_2Fe/Cp_2Fe^+).[5b]

In contrast to the inertness of RRS toward $HSCPh_3$, the addition of 1 equiv of $[Cp_2Fe][BF_4]$ and $HSCPh_3$ into a CH_3CN solution of complex **1** generates the known $[\{Fe(NO)\}^7$-$(\{Fe(NO)_2\}^9)_3]$ $[Fe_4(\mu_3\text{-S})_3(NO)_7]^-$ (RBS) characterized by IR (ν_{NO}) stretching frequencies shifting from (1742 w, 1701 s and 1668 m cm^{-1}) to (1796 w, 1741 s, 1706 w cm^{-1}), and nitric oxide trapped by $[PPN]_2[S_5Fe(\mu\text{-S})_2FeS_5]$ producing the known complex $[PPN][S_5Fe(NO)_2]$ (Scheme 1b).[14] The conversion of complex **1** into RBS triggered by one equiv of S-donor species $HSCPh_3$ and oxidant $[Cp_2Fe][BF_4]$ provided a facile pathway for transformation of RRS into RBS via complex **1**.[1b]

In summary, the assembly of RRS and $\{Fe(NO)_2\}^{10}$ DNIC $[(TMEDA)Fe(NO)_2]$ generating the iron-sulfur nitrosyl cluster **1**, a precursor of Roussin's black salt (RBS), was discovered. Compared to the $\{Fe(NO)_2\}^9$ and $\{Fe(NO)_2\}^{10}$ DNICs/RREs displaying ^{15}N (NO) NMR chemical shift (δ 23 ~ 76 ppm) and (δ -7.8 ~ 25 ppm),[7] respectively, the first semibridging nitroxyl of complex **1** exhibits the distinct ^{15}N (NO) NMR chemical shift (δ 200.8 and 200.1 ppm vs $MeNO_2$). That is, ^{15}N (NO) NMR chemical shift may serve as an efficient tool to discriminate the binding forms of NO (terminal NO vs. semibridging NO and straight M-NO vs. bent M-NO terminal links),[6] in addition to IR ν(NO) spectroscopy (e.g. observed in the diferrous site of an FMN-free FDP (flavodiiron protein) triggering turnover of 2NO to N_2O via a NO-semibridging $Fe^{II}(\mu\text{-NO})Fe^{III}$ intermediate).[4] In this study, we further showed how the electronic structure of the coordinated NO groups of RRS is modulated by the electronic richness of the immediate vicinity $\{Fe(NO)_2\}^{10}$ motifs.

We gratefully acknowledge financial support from the National Science Council of Taiwan. The authors also thank Miss Pei-Lin Chen and Mr. Ting-Shen Kuo for single-crystal X-ray structural determinations.

Notes and references

1 (a) A. R. Butler and I. L. Megson, *Chem. Rev.* 2002, **102**, 1155–1166. (b) K. Szaciłowski, A. Chmura and Z. Stasicka, *Coord. Chem. Rev.* 2005, **249**, 2408–2436.

2 (a) L. Calzolai, Z.-H. Zhou, M. W. W. Adams and G. N. Lamar, *J. Am. Chem. Soc.* 1996, **118**, 2513–2514. (b) D. H. Flint and R. M. Allen, *Chem. Rev.* 1996, **96**, 2315–2334..

3 (a) C. E. Tinberg, Z. J. Tonzetich, H. Wang, L. H. Do, Y. Yoda, S. P. Cramer and S. J. Lippard, *J. Am. Chem. Soc.* 2010, **132**, 18168–18176. (b) Z. J. Tonzetich, H. Wang, D. Mitra, C. E. Tinberg, L. H. Do, F. E., Jr. Jenney, M. W. W. Adams, S. P. Cramer and S. J. Lippard, *J. Am. Chem. Soc.* 2010, **132**, 6914–6916. (c) J. C. Crack, L. J. Smith, M. R. Stapleton, J. Peck, N. J. Watmough, M. J. Buttner, R.

S. Buxton, J. G. Green, V. O. Oganesyan, A. J. Thomson and N. E. Le Brun, *J. Am. Chem. Soc.* 2011, **133**, 1112–1121.

4 T. Hayashi, J. D. Caranto, H. Matsumura, D. M. Jr. Kurtz and P. Moënne-Loccoz, *J. Am. Chem. Soc.* 2012, **134**, 6878–6884.

5 (a) C.-C. Tsou, Z.-S. Lin, T.-T. Lu and W.-F. Liaw, *J. Am. Chem. Soc.* 2008, **130**, 17154–17160. (b) T.-T. Lu, H.-W. Huang and W.-F. Liaw, *Inorg. Chem.* 2009, **48**, 9027–9035. (c) P. P. Paul, Z. Tyeklár, A. Farooq, K. D. Karlin, S. Liu, J. Zubieta, *J. Am. Chem. Soc.* 1990, **112**, 2430–2432.

6 (a) J. Mason, D. M. P. Mingos, D. Sherman and R. W. M. Wardle, *J. Chem. Soc., Chem. Commun.* 1984, 1223–1225. (b) J. Mason, L. F. Larkworthy and E. A. Moore, *Chem. Rev.* 2002, **102**, 913–934.

7 C.-C. Tsou, F.-T. Tsai, H.-Y. Chen, I.-J. Hsu and W.-F. Liaw, *Inorg. Chem.* 2013, **52**, 1631–1639.

8 Z.-S. Lin, T.-W. Chiou, K.-Y. Liu, C.-C. Hsieh, J.-S. K. Yu and W.-F. Liaw, *Inorg. Chem.* 2012, **51**, 10092–10094.

9 (a) C.-C. Tsou, T.-T. Lu and W.-F. Liaw, *J. Am. Chem. Soc.* 2007, **129**, 12626–12627. (b) T.-T. Lu, C.-C. Tsou, H.-W. Huang, I.-J. Hsu, J.-M. Chen, T.-S. Kuo, Y. Wang and W.-F. Liaw, *Inorg. Chem.* 2008, **47**, 6040–6050.

10 (a) A. D. Becke, *Phys. Rev. A* 1988, **38**, 3098−3100. (b) J. P. Perdew, *Phys. Rev. B* 1986, **33**, 8822−8824.

11 M. Kaupp, P. V. R. Schleyer, H. Stoll and H. Preuss, *J. Chem. Phys.* 1991, **94**, 1360−1366.

12 (a) R. Krishnan, J. S. Binkley, R. Seeger and J. A. Pople, *J. Chem. Phys.* 1980, **72**, 650−654. (b) A. J. H. Wachters, *J. Chem. Phys.* 1970, **52**, 1033−1036. (c) P. J. Hay, *J. Chem. Phys.* 1977, **66**, 4377−4384.

13 S. M. Brothers, M. Y. Darensbourg and M. B. Hall, *Inorg. Chem.* 2011, **50**, 8532−8540.

14 M.-L. Tsai, C.-C. Chen, I.-J. Hsu, S.-C. Ke, C.-H. Hsieh, K.-A. Chiang, G.-H. Lee, Y. Wang and W.-F. Liaw, *Inorg. Chem.* 2004, 43, 5159–5167.

Table of content

The fluxional terminal and semibridging NO-coordinate ligands of $[Fe_4(\mu_3\text{-}S)_2(\mu_2\text{-}NO)_2(NO)_6]^{2-}$ are characterized by IR ν(NO), $^{15}N(NO)$ NMR and single-crystal X-ray diffraction.